Delineation of an Active Fragment and Poly(L-proline) II Conformation for Candidacidal Activity of Bactenecin 5†

Periathamby Antony Raj,*,‡,§ Emil Marcus,|| and Mira Edgerton‡,⊥

Department of Oral Biology, Dental Research Institute, Periodontal Disease Clinical Research Center, Department of Prosthodontics, and Department of Biophysical Sciences, State University of New York at Buffalo, 109 Foster Hall, Buffalo, New York 14214

Received July 21, 1995; Revised Manuscript Received December 21, 1995⊗

ABSTRACT: Bactenecin 5 and its fragments [**BN22** (1−22), **BN16** (7−22), and **BC24** (20−43)] were synthesized by solid-phase methods. Their antifungal activities on *Candida albicans* have been studied and compared with those of the native bactenecin 5. The conformational preferences of these peptides in aqueous and nonaqueous solutions and in lipid vesicles were examined by circular dichroism. The highly active N-terminal fragment (**BN16**) was examined in aqueous solution using 500 MHz two-dimensional NMR. Bactenecin 5 and its fragments are potent candidacidal agents against *C. albicans*. The N-terminal fragments (**BN22** and **BN16**) of bactenecin 5 are relatively more active than the C-terminal fragment **BC24**, especially at lower concentrations. The N-terminal region (7−22) which retains the activity of the whole molecule appears to be the functional domain for candidacidal activity. The CD spectra of bactenecin 5 and its fragments are reminiscent of the CD spectrum of poly(L-proline) type II structure in aqueous and nonaqueous solutions and also in lipid vesicles. The temperature dependence of NH chemical shifts and $^1H/^2H$ exchange effect on amide resonances suggest the absence of intramolecularly hydrogen-bonded NH groups. The coupling constant ($J_{NH-C^{\alpha}H}$) values, conformational restriction offered by the Pro residues ($\phi = -60° \pm 15°$), the set of medium- and short-range nuclear Overhauser effects observed for the active N-terminal fragment (**BN16**), and the restrained structure calculation using DIANA suggest that poly(L-proline) type II conformers of the peptide molecules could be significantly populated in aqueous solution. The ability of bactenecin peptides to induce disruption of lipid vesicles correlates well with their activity. Our results suggest that poly(L-proline) type II structure may, indeed, be the biologically active conformation for candidacidal activity of bactenecin peptides.

Bactenecins comprise a family of proline- and arginine-rich antimicrobial polypeptides stored in the granules of bovine neutrophils (Zanetti et al., 1990). They are believed to contribute to the oxygen-independent mechanism of host immune response during phagocytosis (Lehrer et al., 1988). They have been shown to exhibit *in vitro* antibacterial and antiviral activity against a wide variety of microorganisms (Gennaro et al., 1989; Frank et al., 1990). Two polypeptides designated as bactenecin 5 (**Bac 5**)[1] and bactenecin 7 (**Bac 7**) have been isolated. They are believed to be synthesized in immature myeloid cells of the bone marrow and stored as inactive probactenecins in the large granules (Frank et al., 1990; Scocchi et al., 1992). Neutrophil stimulation with microbes has been shown to trigger the removal of the pro region and activation of these peptides (Zanetti et al., 1991). The sequences of **Bac 5** and **Bac 7** have been reported to contain 42 and 59 residues, respectively, on the basis of the primary structure determination using plasma desorption-mass spectrometry (Frank et al., 1990). However, the recent cloning and sequence studies have established a 43-residue sequence as the active form of **Bac 5** (Zanetti et al., 1993). The cidal action of bactenecins has been reported to involve their interaction with the outer membrane of microorganisms (Frank et al., 1990; Zanetti et al., 1990; Vaara, 1992).

Despite the importance of bactenecins in the nonimmune host response, there are relatively few reports on the conformation and structure−function analyses of these bioactive polypeptides (Raj & Edgerton, 1995). Though the mechanism of antimicrobial activity of bactenecins has been ascribed to their interaction with the microbial membranes, the conformations they adopt in the lipid bilayer have not yet been reported. Bactenecins have been shown to exhibit both antibacterial and antiviral activities against several organisms. However, their effects on fungal organisms have not yet been fully studied. In this report, we describe the synthesis, the candidacidal activity, the interaction with lipid bilayers, and the conformational features of bactenecin 5 and its fragments.

† This work was supported by USPHS Research Grants DE08240 and DE04898.

* To whom correspondence should be addressed (telephone, 716-829-2114; FAX, 716-829-3942).

‡ Department of Oral Biology.

§ Dental Research Institute, Periodontal Disease Clinical Research Center.

|| Department of Biophysical Sciences.

⊥ Department of Prosthodontics.

⊗ Abstract published in *Advance ACS Abstracts,* March 15, 1996.

[1] Abbreviations: AMX, spin system of three different protons; ATCC, American Type Culture Collection; CD, circular dichroism; Chol, cholesterol; DIS, denture-induced stomatitis; 2D-NMR, two-dimensional nuclear magnetic resonance; DIANA, distance geometry algorithm for NMR applications; DOPS, dioleylphosphatidylserine; DPPC, dipalmitoylphosphatidylcholine; FID, free induction decay; ^2H_2O, deuterated water; HPLC, high-performance liquid chromatography; NOE, nuclear Overhauser effect; NOESY, NOE spectroscopy; PAGE, polyacrylamide gel electrophoresis; REDAC, redundant dihedral angle constraints; *t*-Boc, *t*-butyloxycarbonyl; TFE, trifluoroethanol; TMP, trimethyl phosphate; TOCSY, total correlated spectroscopy.

0006-2960/96/0435-4314$12.00/0

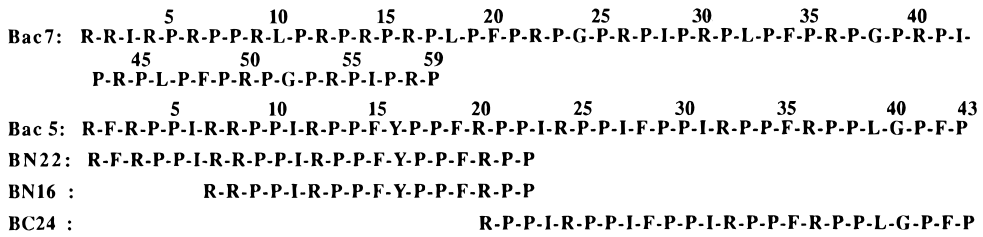

FIGURE 1: Amino acid sequences of bactenecin 7, bactenecin 5, and its fragments. Synthetic bactenecin 5 has the amide function at the C-terminus, whereas the fragments have carboxyl functions. The one-letter symbols used for amino acids in the sequences are described as in IUPAC-IUB Commission on Biochemical Nomenclature (1968).

EXPERIMENTAL PROCEDURES

Selection of Peptides. Bactenecin 5 and its N- and C-terminal fragments (Figure 1) were selected for synthesis as the candidacidal potency of these fragments would serve to delineate the structural requirements for candidacidal activity. The amide function at the C-terminus of **Bac 5** was selected for synthesis as the native molecule has been reported to have an amide group at the C-terminus (Zanetti et al., 1993). However, the carboxyl function at the C-terminus was chosen for the fragments to examine the influence of the C-terminal function on candidacidal activity. The N-terminal fragment (**BN16**) was selected for 2D-NMR studies to determine the structural features of this active sequence which seems to be the functional domain for candidacidal activity.

General Materials and Methods. Chemicals and solvents were of the highest purity available and were used without further purification. Amino acid derivatives, cholesterol (Chol), dipalmitoylphosphatidylcholine (DPPC), dioleylphosphatidylserine (DOPS), and phenylacetamidomethyl and 4-methylbenzhydrylamine resins were purchased from Sigma Chemical Co. (St. Louis, MO) and Bachem (Torrance, CA). All peptides were synthesized using a Beckman System 990 synthesizer. High-performance liquid chromatography (HPLC) was carried out using a Gilson Rabbit-HP system interfaced to an Apple IIe microcomputer. Dried peptide samples were hydrolyzed in sealed tubes for 24 h at 110 °C using 6 N HCl in the presence of 1% phenol vapor, and amino acid analysis was performed on a Beckman System 6300 amino acid analyzer. The amino acid sequences of peptides (∼1 nmol) were checked by sequence analysis using an Applied Biosystems Model 471A protein sequencer interfaced with a Hewlett-Packard HP3394A integrator. The SDS- and cationic-polyacrylamide gel electrophoreses were performed using the methods of Laemmli (1970) and Baum et al. (1977), respectively.

Purification of Native Bactenecin 5. Bovine neutrophils were isolated from freshly collected blood and separated from postnuclear supernatants as described previously (Gennaro et al., 1983). Bactenecin 5 was isolated from the extracts of granules of bovine neutrophils employing ion-exchange and reversed-phase HPLC following the previously reported procedures (Gennaro et al., 1989). Processing of 6.4×10^{10} cells yielded 7.5 mg of bactenecin 5. The purity of the native sequence was examined by reversed-phase HPLC on a Rainin Dynamax-60A analytical C18 column (4.6 × 250 mm) coupled to a guard column (4.6 × 15 mm), as described previously (Raj et al., 1990, 1992). The primary structure of the purified peptide was verified by amino acid and sequence analyses. The homogeneity of the peptide was evaluated by reversed-phase HPLC, SDS-, and cationic-PAGE systems.

Peptide Synthesis and Purification. Bactenecin 5 and its fragments shown in Figure 1 were synthesized by standard solid-phase procedures (Stewart & Young, 1984) using 4-methylbenzhydrylamine and phenylacetamidomethyl resins (for bactenecin 5 and its fragments, respectively) and *N*-*t*-butyloxycarbonyl (*t*-Boc) amino acids as described in our previous publications (Raj et al., 1990, 1992). The side-chain protecting groups were the following: *N*-tosyl (Arg) and *O*-(2-bromobenzyl)oxycarbonyl (Tyr). The coupling reactions were carried out with a 3-fold excess of protected amino acids in a mixture (50% v/v) of *N*,*N*-dimethylformamide and dichloromethane using dicyclohexylcarbodiimide as the coupling reagent in the presence of 1-hydroxybenzotriazole. Completion of the coupling reaction was monitored by the Kaiser test (Kaiser et al., 1970). The *t*-Boc group on the N-terminus was deprotected in 30 min with a 25% solution of trifluoroacetic acid in dichloromethane. The protected peptidyl resin was then treated with anhydrous hydrogen fluoride containing 10% anisole for 1 h at 0 °C. After the hydrogen fluoride was removed, the resin was washed with diethyl ether, the peptide extracted with water containing 1% trifluoroacetic acid, and the aqueous solution lyophilized. The resins containing the C-terminal *t*-Boc-amino acid (0.2−0.3 mmol/g) were used for the synthesis of **Bac 5** and its fragments. The solid-phase synthesis yielded ∼85−90% of the crude peptides. Peptides were purified by reversed-phase HPLC on a Rainin Dynamax-60A C18 column (10 × 250 mm) coupled to a guard column (10 × 50 mm) employing an acetonitrile−water (each containing 0.1% TFA) linear gradient elution (15−50% acetonitrile in water over a period of 60 min) with a flow rate of 2.0 mL min^{-1} (detection at 230 and 225 nm). The fractions of each resolved peak were pooled, lyophilized, and subjected to amino acid and sequence analyses, which identified and verified the authentic peptides. The N-terminal homogeneity and the sequence of the synthetic peptides were verified by amino acid and sequence analyses. The purity of bactenecin 5 and its fragments was also examined in the cationic- and SDS-PAGE systems.

Organisms and Growth Conditions. *Candida albicans* strain ATCC 28366 obtained from the American Type Culture Collection, Rockville, MD, and a clinical isolate from a denture-induced stomatitis (DIS) patient were used. The identity of the clinical isolate was verified by the yeast system (Flow Laboratories, McLean, VA). Organisms were streaked onto Sabouraud dextrose agar plates (Difco Laboratories, Detroit, MI) and maintained at 4 °C. One colony of *C. albicans* from this plate was inoculated into 10 mL of yeast synthetic growth media containing a mixture of $(NH_4)_2SO_4$

(5 g), $MgSO_4 \cdot 7H_2O$ (0.2 g), K_2HPO_4 (2.5 g), NaCl (5 g), sucrose (10 g), and biotin (0.04 g) in 1 L of distilled water (Sundstrom et al., 1987) and incubated for 48 h at 25 °C in a shaker rotating at 200 rpm. After this period the population of yeast cells was in the logarithmic growth phase. The cell morphology was determined and found to be uniformly blastospores by phase contrast microscopy. Subcultures were done every 3 days by inoculating 100 mL of 3-day-old culture into 10 mL of fresh synthetic media.

Measurement of Candidacidal Activity. The antifungal activity of the **Bac 5** and its fragments was assessed *in vitro* against *C. albicans*. The loss of cell viability has been expressed as a function of peptide concentration. The assay was performed as described in the candidacidal activity of salivary histatin 5 and its fragments (Raj et al., 1990). We refer to the candidacidal action of peptides as a loss of viability of cells, since the inability of the yeast to replicate following removal of peptides indicates nonviability. Thus, the assay used in this study measured only fungicidal activity. The candidacidal activity of bactenecin 5 and its fragments has been found to be influenced by peptide concentration and incubation time. The time-dependent loss of viability of cells induced by **Bac 5** and its fragments at different concentrations has shown that maximal loss in cell viability could be reached within 50 min after incubation for all peptides. Cells from 48 h cultures were harvested, washed, and resuspended to a concentration of 5×10^7 cells/mL in 0.01 M sodium phosphate buffer (pH 7.4). Stock solutions of peptides (range 0.375−500 μM) to be tested were made in 0.01 M sodium phosphate buffer. Peptide concentrations were determined by amino acid analysis. A microassay system was utilized in which 100 μL of the stock solution of test peptide was incubated with 100 μL (5×10^6 cells) of yeast suspension in sterile glass test tubes at 37 °C for 1 h. Control suspensions of 100 μL of cells and 100 μL of sodium phosphate buffer were incubated simultaneously. Each tube of cell suspension was shaken for 10 s every 15 min during this time. A 100 mL aliquot of cells was removed from the tube, diluted to 5×10^2 cells/mL in sodium phosphate buffer, and then vortexed. Aliquots of 0.5 mL of each suspension were spread onto plates (15 × 100 mm) of Sabouraud dextrose agar in duplicate. *C. albicans* was grown overnight at 37 °C, and candidacidal activity of the test peptide was assessed as the ratio of colonies per test plate to the number of colonies on control (no peptide) plates.

Vesicle Preparation and Fluorescence Measurements. Unilamellar lipid vesicles [dipalmitoylphosphatidylcholine (DPPC):dioleylphosphatidylserine (DOPS), or DPPC:cholesterol in 3:1 ratios] encapsulated with the fluorescent dye calcein were prepared by the reversed-phase evaporation procedures (Straubinger & Papahadjopoulos, 1982) using 20 mL of phospholipid (50 mg), 2 mL of diethyl ether, and 1 mL of an aqueous solution (150 mM sodium chloride and 10 mM TES at pH 7.5) containing 25 mM calcein as described previously (Straubinger & Papahadjopoulos, 1982). Unencapsulated calcein was removed by passing through a Sephadex G-50−80 column equilibrated with the buffer at room temperature. The liposomes were then extruded through a 0.1 mm polycarbonate membrane, applying a high-pressure extruder to obtain uniformly sized vesicles. Samples were prepared by dilution of the liposomes to 0.1 mg/mL in the above-mentioned buffer solution. Peptides in water were prepared at varying concentrations (2−10 μM), and aliquots were added to 0.5 mL of liposome solutions. The samples were incubated at 25 °C for 15 min and then analyzed for fluorescence change.

The peptide-induced lysis of lipid vesicles was monitored by measuring the dequenching of fluorescence caused by the leakage of calcein which is encapsulated at self-quenching concentrations inside the liposomes. The fluorescence intensity was measured at 520 nm by excitation at 495 nm as a function of time for 15 min using a Perkin-Elmer 650-40 fluorescence spectrophotometer. Complete release of calcein was obtained by lysing the vesicles with Triton X-100. The percent lysis was calculated from the equation % lysis $= [I_o - I_b/I_t - I_b] \times 100$, where I_o is the observed fluorescence, I_b is the background fluorescence, and I_t is the fluorescence after the addition of Triton X-100.

Circular Dichroism. CD spectra were recorded at 30 °C with a JASCO J-600 spectropolarimeter interfaced to an IBM PS/2 microcomputer. It has been ascertained that the total absorbance of the cell, solvent, and sample is lower than 1.0 before the CD spectrum was recorded. Measurements were carried out in a cylindrical quartz cell (Helma, Jamaica, NY) with a 0.05 mm path length using a peptide concentration of 0.1−0.3 mM. CD spectra were recorded at 30 °C using a 1.0 nm bandwidth, a scanning rate of 10 nm/min with a wavelength step of 0.2 nm, and a time constant of 2 s. The temperature control was achieved by circulating water through a cell jacket. The peptide in an aqueous DPPC dispersion was prepared by a method similar to that described previously (Epand et al., 1987). The lipid DPPC (7.0 mM) was dissolved in chloroform and dried under a stream of nitrogen and then under vacuum to form a thin film on the surface of a round-bottomed flask. The peptide (0.35 mM) dissolved in 10 mM sodium phosphate buffer (pH 7.4) was added, vortexed, sonicated using a bath-type sonicator, and incubated at 50 °C (above the phase transition of the lipid) for 4 h. The lipid peptide molar ratio was 20:1. CD band intensities are expressed as molar ellipticities, $[\theta]_M$, in $deg \cdot cm^2 \cdot dmol^{-1}$.

NMR Measurements. The purified **BN16** (7 mg) was dissolved in 630 μL of double distilled water and 70 μL of ^2H_2O (Cambridge Isotope Laboratories, Woburn, MA). All 1D- and 2D-NMR experiments used for conformational analysis were performed at 30 °C. All NMR experiments were carried out at 500 MHz on a Varian VXR-500 spectrometer equipped with a SUN Sparcstation 2. The 1D-NMR spectra were recorded with a spectral width of 5000 Hz and a relaxation delay time of 2.5 s using 8K data points, zero filled to 32K before Fourier transformation. All 2D-NMR spectra were acquired in the phase-sensitive absorption mode with quadrature detection in both dimensions using the hypercomplex method (States et al., 1982). Typically, 2048 complex data points during the acquisition time (t_2) and 256−512 complex FIDs during the evolution period t_1 with a total of 48−64 transients for each FID were collected. The spectral width in both dimensions was 4500 Hz for the 500 MHz data. The solvent signal of water was suppressed by low-power irradiation of the resonances at all times except during t_1 and t_2. All 2D experiments were multiplied by a phase-shifted sine-bell function in both dimensions and zero filled prior to Fourier transformation to achieve appropriate resolution in each dimension. The TOCSY experiments (Braunschweiler & Ernst, 1983; Bax et al., 1984) were recorded using a MLEV-16 pulse sequence for the spin lock

with a field strength of approximately 5.6 kHz and a trim pulse of 2 ms using an isotropic mixing period of 65 ms. The 2D-NOE experiments (Jeener et al., 1979; Kumar et al., 1980; Wüthrich, 1986) were performed with a mixing time of 150 ms after ascertaining that spin diffusion is not significant at this mixing time. The coupling constant ($J_{NH-C^{\alpha}H}$) values were determined from the 1D spectrum with a high digital resolution of 0.1 Hz, since the NH resonances of the peptide are well resolved.

Hydrogen−deuterium ($^1H/^2H$) exchange of the amide groups was studied using 65% ^2H_2O in aqueous solution, recording the 1D spectrum immediately. Variable temperature experiments have been recorded between 283 and 323 K, and the temperature was maintained by a Varian/Oxford temperature control unit with a sensitivity of ±0.2 K. The NH chemical shits varied linearly (high-field shift) with increasing temperature. The temperature coefficients ($d\delta/dT$) of amide chemical shifts were determined as the order of 10^{-3} ppm K^{-1}.

Structure Calculation. The $^1H-^1H$ distances for structure determination were obtained from NOE cross-peak intensities in the 2D-NOESY spectrum obtained with 150 ms mixing time. We selected the $C^{\beta}H/C^{\beta}H'$ cross peak of Phe_9 as the reference to calibrate the intensities against known distances. Dihedral ϕ angle restraints were obtained from the coupling constant ($J_{NH-C^{\alpha}H}$) values via the Karplus equation (Pardi et al., 1983).

Structures were initially generated using the variable target function algorithm DIANA including REDAC (Güntert et al., 1991; Güntert & Wüthrich, 1991). The ϕ angle restraints deduced from $J_{NH-C^{\alpha}H}$ and all upper distance restraints calculated from the NOESY spectrum [a total of 58 NOE constraints [$d_{\alpha N}$ (i, i+1), $d_{\alpha N}$ (i, i), $d_{\alpha\delta}$ (i, i+1), $d_{\beta N}$ (i, i), $d_{\alpha\alpha}$ (i, i+1), and side-chain interproton distances] were used as the starting parameters for the DIANA calculations. Computations were carried out using standard minimization parameters (Güntert & Wüthrich, 1991), and 16 DIANA structures with the lowest target function were selected. These structures were subsequently subjected to restrained energy minimization consisting of 500 iterations with the application of conjugate gradients (Powell, 1977), employing the AMBER force field (Weiner et al., 1984, 1986) until the root mean square gradient was smaller than 0.05 kcal mol^{-1} $Å^{-2}$. During minimization electrostatic interactions were taken into account with a distance-dependent dielectric function. Distance geometry calculations were performed on a Silicon Graphics 4D/35 workstation. Restrained energy minimization and structures analysis were carried out using the SYBYL 5.52 molecular modeling package (Tripos Associates, Inc., St. Louis, MO) on an Evans & Sutherland ESV3 workstation.

RESULTS

Peptide Synthesis. The solid-phase method used for the synthesis of **Bac 5** and its fragments yielded 60−65% of pure peptides after HPLC purification. The amino acid and sequence analyses have been found to be consistent with their primary structures. The HPLC retention time and the cationic- and SDS-PAGE analyses (Figure 2) established the identity of synthetic **Bac 5**. The CD spectra of synthetic **Bac 5** are similar to those of the natural molecule, suggesting the optical purity of the synthesized peptide (Figure 3).

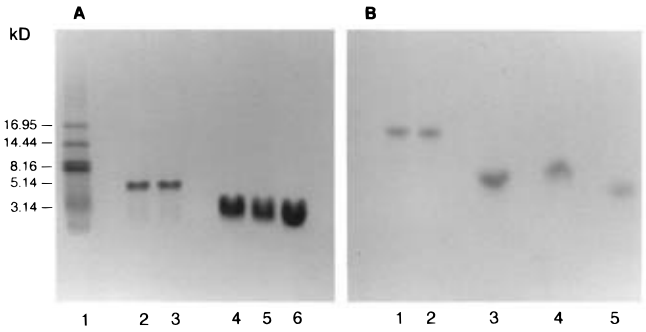

FIGURE 2: (A) SDS (15%)-PAGE of bactenecin 5 and its fragments under reducing conditions. Lanes 1, 2, 3, 4, 5, and 6 correspond to molecular mass standards (10 μg), synthetic **Bac 5** (5 μg), natural **Bac 5** (5 μg), **BC24** (5 μg), **BN22** (5 μg), and **BN16** (5 μg) respectively. (B) Cationic (15%)-PAGE of bactenecin 5 and its fragments. Lanes 1, 2, 3, 4, and 5 correspond to synthetic **Bac 5** (5 μg), natural **Bac 5** (5 μg), **BC24** (5 μg), **BN22** (5 μg), and **BN16** (5 μg), respectively. Electrophoresis was carried out using a Mini Gel apparatus (Hoeffer Scientific Instruments, San Francisco, CA). The gels were stained with 0.1% Coomassie blue.

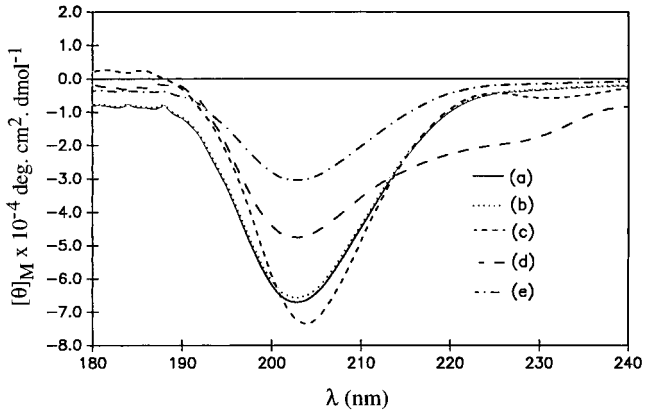

FIGURE 3: CD spectra of synthetic and native bactenecin 5 recorded at 30 °C: (a) synthetic **Bac 5** in sodium phosphate buffer at pH 7.4; (b) native **Bac 5** in sodium phosphate buffer at pH 7.4; (c−e) synthetic **Bac 5** in trifluoroethanol (c), trimethyl phosphate (d), and DPPC vesicles (e) (peptide:lipid molar ratio 1:20).

Table 1: Percent Loss of Viability of *C. albicans* (DIS) Induced by Bactenecin 5 and Its Fragments[a]

	loss of viability (%)[b]				
concn (μM)	**BN16**	**BN22**	**BC24**	**Bac 5** (synthetic)	**Bac 5** (native)
250	100 ± 0	99 ± 1	99 ± 1	100 ± 0	100 ± 0
100	99 ± 1	95 ± 1	95 ± 1	97 ± 2	99 ± 2
50	93 ± 4	95 ± 2	89 ± 4	95 ± 2	99 ± 2
25	86 ± 6	85 ± 8	65 ± 10	82 ± 4	85 ± 5
10	53 ± 10	51 ± 8	27 ± 8	53 ± 7	56 ± 8
5	30 ± 11	25 ± 12	5 ± 2	25 ± 10	30 ± 12
EI_{50} (μM)[c]	9.1 ± 1.2	9.8 ± 2.4	19.4 ± 2.0	9.2 ± 0.5	9.1 ± 0.6

[a] Values are expressed as means ±SD based upon three separate experiments, each run in duplicate. [b] Expressed as [1 − (cell survival after peptide incubation)/(cell survival in buffer alone)] × 100. [c] EI_{50} = peptide concentration (μM) required to induce half-maximal loss in cell viability as determined for the concentration effect curve.

Candidacidal Activity. The efficacy of bactenecin 5 and its fragments to induce loss of viability of *C. albicans* was measured at various peptide concentrations, and the results are summarized in Table 1. The EI_{50} [peptide concentration (μM) which would induce half-maximal loss in cell viability] values for these peptides are also provided in Table 1. The data provided in Table 1 are for the DIS strain. The *C.*

Table 2: CD Parameters for Bactenecin 5 and Its Fragments

	phosphate buffer (pH 7.4)		trifluoroethanol		trimethyl phosphate		DPPC[b]	
peptide[a]	λ (nm)	$[\theta]_M \times 10^{-3}$ [c]	λ (nm)	$[\theta]_M \times 10^{-3}$	λ (nm)	$[\theta]_M \times 10^{-3}$	λ (nm)	$[\theta]_M \times 10^{-3}$
Bac 5 (synthetic)	202	−67.09	202	−47.43	203	−30.49	204	−73.54
	231 (198)	−3.14 (−57.25)	224	−20.39	235	−1.13	231	−5.80
Bac 5 (native)	202	−65.78	202	−48.12	203	−30.25	204	−74.68
	231	−3.07	224	−20.54	235	−2.25	231	−6.26
BC24 (20−43)	202	−34.02	202	−26.29	203	−25.37		
	228 (198)	−0.92 (−25.34)	224	−11.58	234	−1.03		
BN22 (1−22)	202	−28.77	202	−21.91	203	−26.13		
	229 (198)	1.03 (20.43)	224	−5.96	232	−0.82		
BN16 (7−22)	203	−28.50	202	−21.83	203	−19.52		
	228 (198)	1.52 (−20.36)	227	−4.10	228	+1.25		

[a] Peptide concentration 0.1−0.3 mM. [b] Peptide:lipid molar ratio 1:20. [c] $[\theta]_M$ expressed as deg·cm^2·dmol^{-1}. The λ and $[\theta]_M$ within parentheses correspond to the $\pi-\pi^*$ band at 45 °C.

albicans strain 28366 has been found to be 10−20% more susceptible to these peptides. Peptide concentration influences both the rate and the candidacidal activity. The activity data of synthetic **Bac 5** are consistent with those of the native molecule (Table 1). The cidal potency of all fragments is comparable to that of the parent molecule at higher peptide concentrations. However, the candidacidal activity of the C-terminal sequence (**BC24**) appears to be relatively less than the N-terminal fragments and the parent molecule as shown by the EI_{50} values (Table 1). Compared to **Bac 5** and its N-terminal sequences, **BC24** has less positive charge at the N-terminal end (Figure 1). Hence, the diminished activity observed for **BC24** suggests that the basic residues (Arg) at the N-terminus may be important for high cidal potency. The amide function at the C-terminus of **Bac 5** may not be essential for activity, as the cidal activity of the N-terminal fragments which have carboxyl function is comparable to the parent molecule. The cidal potencies of **BN16** and **BN22** at various peptide concentrations are comparable, indicating that the first six residues (R-F-R-P-P-I) at the N-terminus of **BN22** (Figure 1) may not be essential for candidacidal activity. The cidal activities of **Bac 5** and **BN16** over the concentration range of 5−100 μM (Table 1) appear almost identical, suggesting that **BN16** (7−22 of **Bac 5**) could be the functional domain for the candidacidal activity of bactenecin 5.

Peptide-Induced Disruption of Lipid Membranes. The peptide-induced lysis of lipid vesicles has been monitored by measuring the dequenching of fluorescence caused by the leakage of calcein, which is encapsulated at self-quenching concentrations inside the liposomes. The lytic effect of **Bac 5** and its fragments on neutral and negatively charged liposomes, DPPC:cholesterol and DPPC:DOPS, respectively, is shown in Figure 4. The efficacy of **Bac 5** and its fragments to disrupt the neutral lipid (DPPC:cholesterol) appears minimal (Figure 4B). In contrast, **Bac 5** and its fragments strongly interact with the negatively charged liposomes, indicating that electrostatic forces could primarily mediate peptide-membrane interaction. **Bac 5** and its N-terminal fragments induce nearly 75% lysis of the negatively charged vesicles within 10 min after incubation, whereas the C-terminal fragment **BC24** exhibits less lytic effect (Figure 4A). The diminished lytic effect observed for **BC24** could be due to the decrease in the positive charge at the N-terminus of this peptide. The results suggest that the initial interaction could involve electrostatic forces between the positively charged residues at the N-terminus and the negatively charged lipid bilayer.

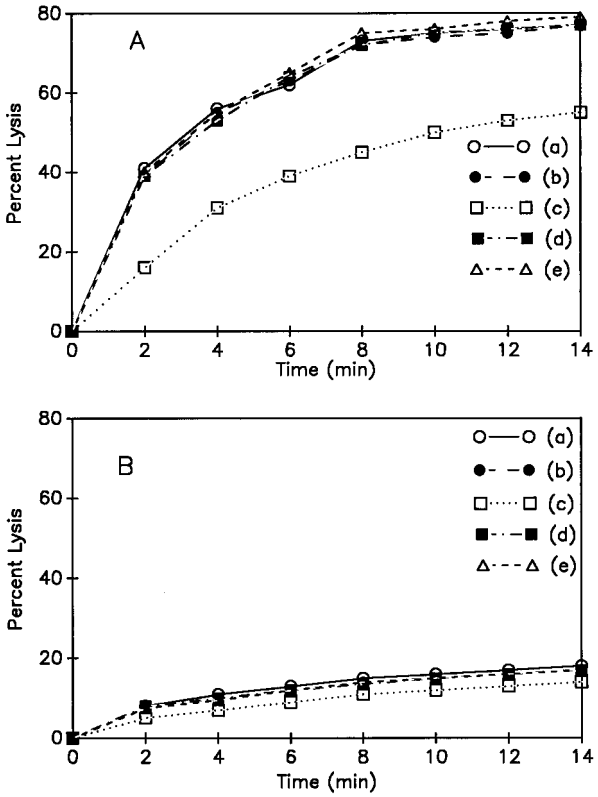

FIGURE 4: Lytic effect of synthetic **Bac 5** (a), native **Bac 5** (b), **BC24** (c), **BN22** (d), and **BN16** (e) on DPPC:DOPS (A) and DPPC:Chol (B) liposomes containing the fluorescent probe calcein. A peptide concentration of 10 μM was used.

Circular Dichroism Studies. The CD spectra of bactenecin 5 and its fragments in 10 mM sodium phosphate buffer at pH 7.4, trifluoroethanol (TFE), and trimethyl phosphate (TMP) are provided in Figures 3 and 5, and the CD parameters are provided in Table 2. The CD spectrum of synthetic **Bac 5** shows a strong broad negative $\pi-\pi^*$ band at ~203 nm ($[\theta]_M = -67.09 \times 10^3$ deg·cm^2·dmol^{-1}) with the n$-\pi^*$ band at ~231 nm ($[\theta]_M = -3.14 \times 10^3$ deg·cm^2·dmol^{-1}) in aqueous solution. The CD data of synthetic **Bac 5** in phosphate buffer (Figure 5) and the data provided in Table 2 are in good agreement with those of the native sequence. In TFE and TMP, the peptide retains the strong negative band around ~202−204 nm ($[\theta]_M = -47.66 \times 10^3$ deg·cm^2·dmol^{-1} and $[\theta]_M = -30.05 \times 10^3$ deg·cm^2·dmol^{-1}, respectively). The CD spectra of the fragments of bactenecins provided in Figure 5 also resemble the CD spectra of **Bac 5**. However, the ellipticity values of

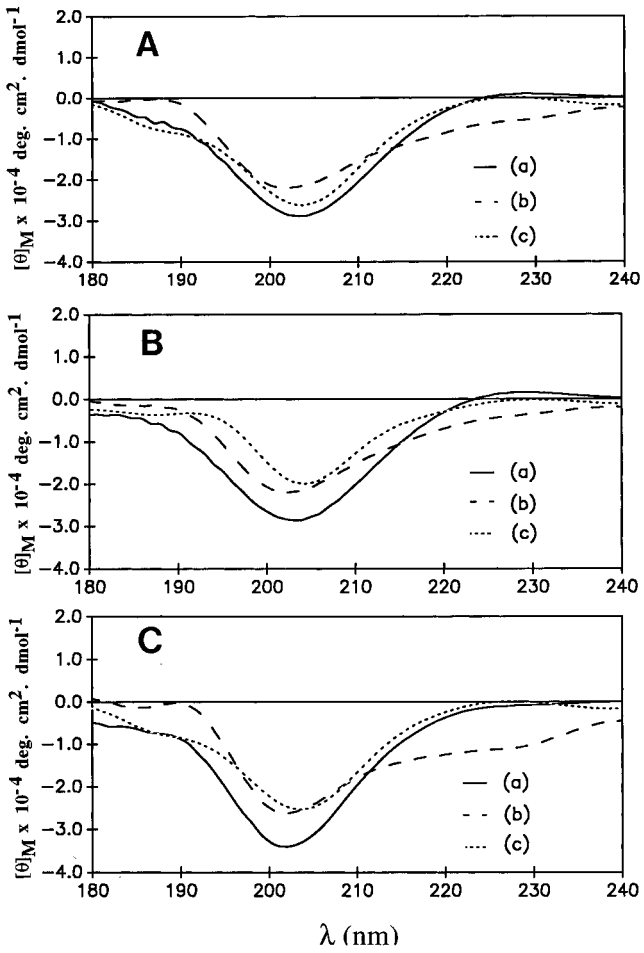

FIGURE 5: CD spectra of **BN22** (A), **BN16** (B), and **BC24** (C) in (a) sodium phosphate buffer at pH 7.4, (b) trifluoroethanol, and (c) trimethyl phosphate.

the strong negative $\pi-\pi^*$ band are lower than those of the whole molecule. The lowered ellipticity values observed for the fragments of bactenecins could be attributed to their shorter chain length as compared to the whole molecule. Such diminished ellipticity values, as a consequence of decreased peptide chain length, have been observed and reported for helical peptides (Vijayakumar et al., 1984), fragments of salivary histatin 5 and statherin (Raj et al., 1990, 1992). A strong negative band at ∼206 nm with a weak positive band at ∼229 nm is characteristic of the poly (L-proline) II helical structure (Ronish & Krimm, 1974; Loomis et al., 1985; Rabanal et al., 1993). The absence of the weak positive band expected for the poly(L-proline) II helix and the shift in the strong negative $\pi-\pi^*$ band from ∼206 to 202 nm may be due to the presence of only one-half of the tertiary amide groups (Woody, 1992) or due to a slight deviation from the ideal poly(L-proline) II ($\phi = -78°$; $\psi = 145°$; $\omega = 180°$) helical conformation (Arnott & Dover, 1968). The presence of minor populations of *cis* conformations [poly(L-proline) I, $\omega = 0°$] may also cause a change in the positive n$-\pi^*$ transition and a shift in the $\pi-\pi^*$ transition toward shorter wavelength. The presence of a population of *cis* conformations is common in proline-rich peptides, as the energy difference expected between the *cis* ($\omega = 0°$) and the *trans* ($\omega = 180°$) conformations is small (Carver & Blout, 1977). The contribution of aromatic residues (Phe and Tyr) to the CD n$-\pi^*$ transition might have also altered the positive ellipticity normally observed for the poly(L-proline) II helical conformation. Though the overall band shape of these proline-rich peptides in different solvents remains unaffected, change in the intensity of both the n$-\pi^*$ and $\pi-\pi^*$ bands is observed (Figures 3 and 5), suggesting the structural flexibility of these linear sequences. Such perturbation in the CD spectra of poly(proline) helices caused by solvents has previously been reported (Rabanal et al., 1993). The CD spectrum of bactenecin 5 in DPPC vesicles (Figure 3) indicates an increase in the intensity of the $\pi-\pi^*$ transition and a shift in the band position toward the longer wavelengths as compared to that in phosphate buffer. This suggests that peptide molecules may associate in the lipid bilayer to form a higher order poly(proline) helical structure.

A 5-fold increase or decrease in the peptide concentration in aqueous solutions does not significantly alter the CD band intensities, indicating that peptide association is not significant at the concentrations used for CD measurements. Increase of temperature (>40 °C) causes a red shift in the CD bands with a significant decrease in the $\pi-\pi^*$ ellipticity values. This temperature effect has been commonly observed in proline-rich oligo- and polypeptides and interpreted in terms of a transition from the poly(proline) II helix to disordered random coil (Tiffany & Krimm, 1972; Rabanal et al., 1993).

The recent circular dichroic analysis of polyproline II helices has identified indistinguishable CD spectra corresponding to poly(proline) II segments of at least two residues or all residues (Sreerama & Woody, 1994). Though the CD spectra of **Bac 5** and its fragments are characteristic of poly(proline) II structure, it is not be possible to distinguish whether the CD contribution is from the population of fully extended poly(proline) II structures or from conformations defined by segments of two or more residues. The CD data can also be interpreted by structures with Pro-Pro dipeptide segments in the poly(proline) II state, while the non-proline residues remain in the random conformation. In order to distinguish these possibilities, the biologically active fragment **BN16** was examined by 2D-NMR studies.

NMR Studies. The shorter fragment **BN16** has been selected for NMR studies as its candidacidal potency is comparable to that of bactenecin 5. Moreover, its CD band shapes in different solvents are similar to those of bactenecin 5. The 500 MHz ^{1}H-NMR spectrum of **BN16** recorded in aqueous solution (pH 3.8) at 30 °C exhibits well-resolved amide resonances except for Phe_9 and Tyr_{10} (Figure 6). The NH, C$^\alpha$H, and the side-chain phenyl and methyl resonances are distinctly sharp at 30 °C. The line width of these resonances remain unaltered even when the temperature is lowered to 10 °C (Figure 6b). These observations suggest that over the temperature range 10−30 °C the NMR spectral parameters are dominated by contributions from a major population of conformers. A 5-fold dilution of the peptide does not show any change both in the chemical shift of NH and C$^\alpha$H resonances and in their line widths, indicating that peptide association is not significant at the concentration used for NMR studies. At 40 °C the line width of all NH resonances are broad (Figure 6d), suggesting chemical exchange across conformational species. The observed ^{1}H-NMR resonances at 30 °C are due to a major population (95%) of nearly exclusively *trans* prolines. Additional peaks could be observed in the spectrum represented by a very weak population of *cis* prolines (5%) as determined from the integrated intensity of the resonances. Conformational

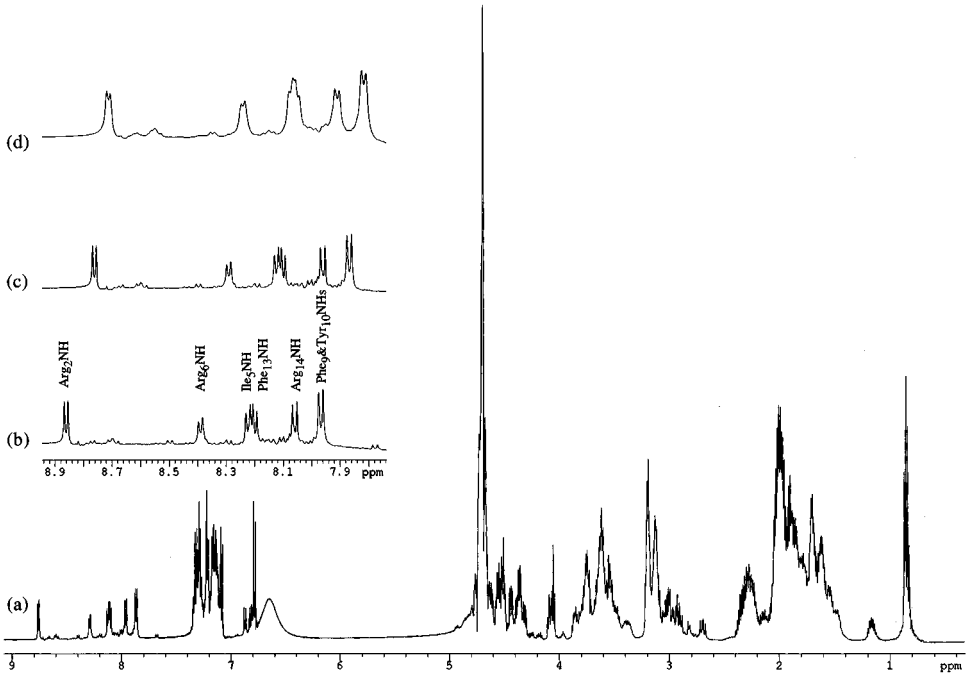

FIGURE 6: 500 MHz ^{1}H-NMR spectrum of **BN16** in $H_2O/^2H_2O$ recorded at 30 °C (a) with NH resonances at 10 °C (b), 30 °C (c), and 40 °C (d).

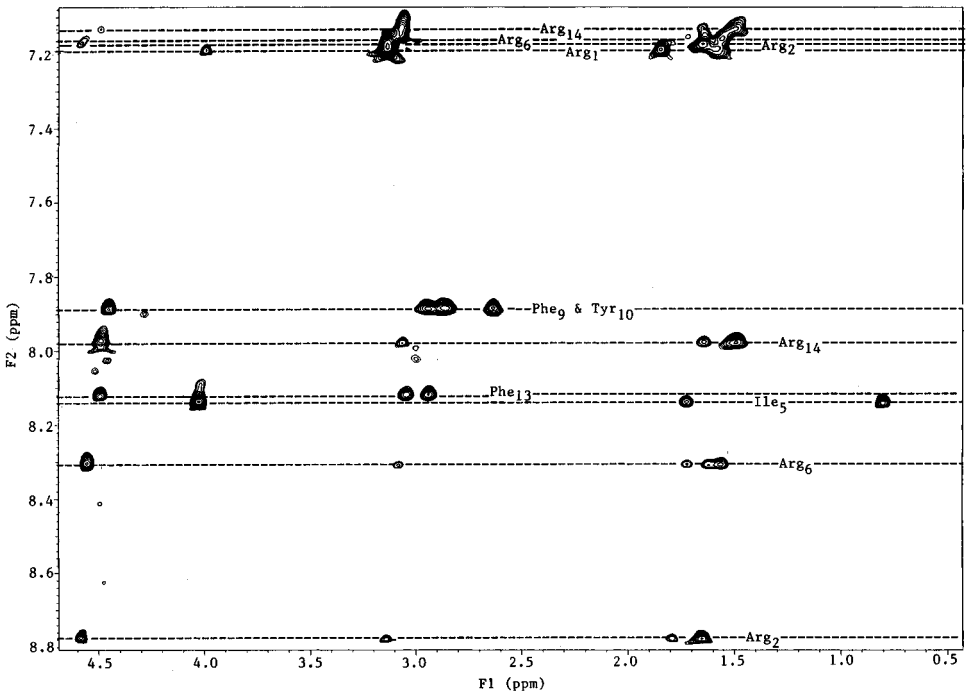

FIGURE 7: Part of the TOCSY spectrum of **BN16** showing the backbone amide and Arg side-chain amino resonance connectivities to $C^{\alpha}H$, $C^{\beta}H$, $C^{\gamma}H$, and $C^{\delta}H$ resonances. The spectrum was recorded in $H_2O/^2H_2O$ at pH 3.8 and 30 °C.

analysis has been carried out only for the major *all-trans* peptide molecules.

*Resonance Assignments of **BN16**.* The resonance assignments of the ^{1}H NMR spectrum of the **BN16** fragment in water were made by the standard sequential assignment procedures (Wüthrich, 1986) and accomplished by the combined analyses of the 2D-TOCSY and 2D-NOE spectra. The 2D-TOCSY spectra were also recorded at different temperatures (283−323 K) to assign unambiguously the overlapping connectivities. The amide connectivities to the side-chain protons in the TOCSY spectrum are provided in Figure 7. The identification of most of the spin system was made from the amide proton TOCSY connectivities (Figure 7). One of the arginines has been unambiguously assigned to the N-terminal Arg_1, which exhibits only one series of connectivity of its side-chain proton resonances to the side-chain amino proton resonance (Figure 7). The other three arginine residues have been readily recognized by two distinct series of connectivities of their side chains to the backbone amide (Figure 7). The Ile_5 was identified from the occurrence of $C^{\delta}H_3$ at δ 0.8 ppm and its connectivities to $C^{\gamma}H$, $C^{\beta}H$, and backbone amide proton resonances. In addition, three AMX spin systems whose $C^{\beta}H$ resonances occur at δ 2.64−3.04 ppm corresponding to two Phe (Phe_9

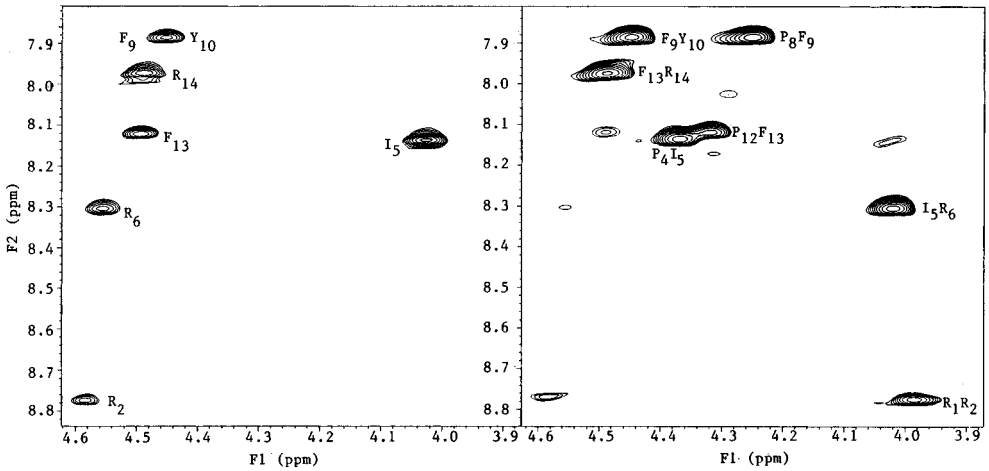

FIGURE 8: Fingerprint regions in the TOCSY (left) and NOESY (right) spectra of **BN16** in $H_2O/^2H_2O$ at pH 3.8 and 30 °C. The αN connectivities in the TOCSY and αN (*i*, *i*+1) connectivities in the NOESY spectra are labeled.

and Phe_{13}) residues and one Tyr (Tyr_{10}) residue were also identified in the TOCSY spectrum.

The assignment of resonances to individual amino acids was accomplished by the analysis of the $C^{\alpha}H-NH$ connectivities in the fingerprint regions in the TOCSY and NOESY spectra. The fingerprint regions of the TOCSY and NOESY spectra are provided in Figure 8. The Arg NH (δ 8.31 ppm) which gives a strong NOE to Ile_5 $C^{\alpha}H$ at δ 4.03 ppm (Figure 8) has been assigned to Arg_6. The Arg NH at δ 7.98 ppm gives a strong NOE to $C^{\alpha}H$ of an aromatic residue at δ 4.49 ppm, which has been unambiguously assigned to Phe_{13} $C^{\alpha}H-Arg_{14}$ NH connectivity. The other Arg NH at δ 8.77 ppm has been assigned to Arg_2 and confirmed by its NOE connectivity to Arg_1 $C^{\alpha}H$ at δ 3.99 ppm, which does not show any backbone amide connectivity in the TOCSY spectrum (Figure 7). The Pro $C^{\alpha}H$ at δ 4.25 ppm shows a connectivity to NH of an aromatic residue at δ 7.89 ppm, which could be safely assigned to the αN connectivity between Pro_8 and Phe_9 residues. Since Phe_9 and Phe_{13} NH resonances have already been assigned, the other aromatic NH resonance at δ 7.89 ppm has been assigned to Tyr_{10}. The NOE connectivities between the aromatic ring and the $\alpha\beta$ protons have been used to assign the respective ring protons to individual residues.

The αN (*i*, *i*+1) connectivities observed for Ile_5, Phe_9, and Phe_{13} NHs allowed unambiguous assignments of $C^{\alpha}H$ resonances of Pro_4, Pro_8, and Pro_{12}, respectively. The respective $C^{\beta}H$, $C^{\gamma}H$, and $C^{\delta}H$ resonances were identified from the TOCSY spectrum. The $C^{\alpha}H-C^{\delta}H$ (*i*, *i*+1) NOE connectivities of Arg_2-Pro_3, Arg_6-Pro_7, Tyr_{10}-Pro_{11}, and Arg_{14}-Pro_{15} have been used to identify the resonances of Pro_3, Pro_7, Pro_{11}, and Pro_{15} residues. The Pro_{15} $C^{\alpha}H$ at δ 4.46 ppm shows a strong NOE to the $C^{\delta}H$ resonance at δ 3.65 ppm, which has been assigned to Pro_{16} $C^{\delta}H$. Thus, by the combined use of TOCSY and NOESY spectra, resonances have been assigned to individual residues. The protons of the N-terminal amino group, the C-terminal carboxyl group, and the hydroxyl group of Tyr_{10} were not identified, presumably due to their fast exchange with the solvent protons. The chemical shifts of all the assigned protons in water are listed in Table 3.

Conformational Analysis in Aqueous Solution. A summary of NMR and NOE parameters is provided in Figure 9. A set of characteristic strong, medium, and weak NOE connectivities, $J_{NH-C^{\alpha}H}$ values, temperature coefficients of NH chemical shifts, and fast $^1H/^2H$ exchange of amide groups have been considered as criteria to examine whether the **BN16** linear sequence has any preferred backbone conformation in aqueous solution. The temperature coefficients of

Table 3: ^1H Chemical Shifts (ppm)[a] of the Bioactive Fragment (**BN16**) of Bactenecin 5 in $H_2O/^2H_2O$ at 30 °C, pH 3.8

residue	NH	$C^{\alpha}H$	$C^{\beta}H$	$C^{\gamma}H$	others
Arg_1		3.99	1.85	1.59	$C^{\delta}H$ 3.13; $N^{\delta}H$ 7.19
Arg_2	8.77	4.58	1.79	1.65	$C^{\delta}H$ 3.14; $N^{\delta}H$ 7.17
Pro_3		4.29	2.05	1.92	$C^{\delta}H$ 3.76/3.68
Pro_4		4.37	2.19	1.94/1.81	$C^{\delta}H$ 3.70/3.56
Ile_5	8.14	4.03	1.72	1.11/1.02	$C^{\delta}H$ 0.8
Arg_6	8.31	4.56	1.72	1.62, 1.56	$C^{\delta}H$ 3.08; $N^{\delta}H$ 7.16
Pro_7		4.33	2.17	1.93/1.79	$C^{\delta}H$ 3.70/3.56
Pro_8		4.25	2.21/2.09	2.03/1.94	$C^{\delta}H$ 3.69/3.52
Phe_9	7.89	4.45	2.94, 2.86		$C^{\delta}H$ 7.13; $C^{\epsilon}H$ 7.24; $C^{\zeta}H$ 7.36
Tyr_{10}	7.89	4.45	2.76, 2.64		$C^{\delta}H$ 7.10; $C^{\epsilon}H$ 6.82
Pro_{11}		4.48	2.27	1.93	$C^{\delta}H$ 3.54/3.49
Pro_{12}		4.32	2.21/1.97	1.89/1.76	$C^{\delta}H$ 3.82/3.68
Phe_{13}	8.12	4.49	3.04, 2.94		$C^{\delta}H$ 7.14; $C^{\epsilon}H$ 7.26; $C^{\zeta}H$ 7.34
Arg_{14}	7.98	4.47	1.64	1.49	$C^{\delta}H$ 3.06; $N^{\delta}H$ 7.14
Pro_{15}		4.46	2.26	1.93	$C^{\delta}H$ 3.56/3.47
Pro_{16}		4.39	2.18	1.90	$C^{\delta}H$ 3.65/3.56

[a] Chemical shifts were determined ±0.02 ppm relative to the proton resonance of $H_2O/^1HO^2H$ at 4.7 ppm.

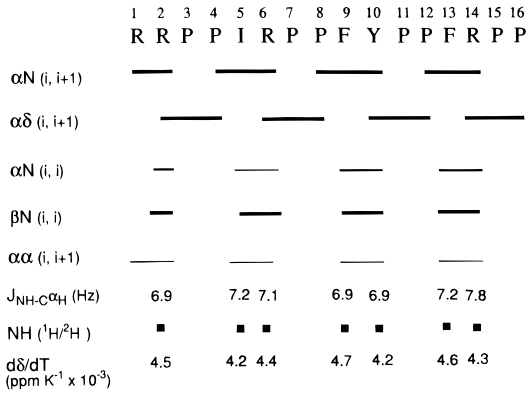

FIGURE 9: Summary of sequential and medium-range NOE data compiled from the NOESY spectra of **BN16** recorded at 30 °C in $H_2O/^2H_2O$. The thickness of the bars indicates that the NOE is strong, medium, and weak, respectively. ■ indicates fast exchanging amide NHs.

all amide resonances provided in Figure 8 are high ($\geq$0.0042 ppm K^{-1}), suggesting that the backbone NH groups are well exposed to the solvent and not involved in any intramolecular hydrogen-bonding interactions. In 65% ^2H_2O, the amide protons of all non-proline residues were exchanged within 45 min. The $^1H/^2H$ exchange rate observed for all backbone amide resonances (Figure 9) provides further evidence that the amide NH groups are not involved in any intramolecular hydrogen bonding in aqueous solution.

The strong $\alpha\delta$ (i, i+1) NOE connectivities observed between proline and its preceding non-proline residues and between two adjacent proline residues suggest the presence of nearly exclusively *trans* prolines. These observations indicate that the backbone ω angles for all residues fall at $\pm$180°. The αN and $\alpha\delta$ (i, i+1) distances are dependent on the dihedral angle ψ_i (Shenderovich et al., 1984; Wüthrich et al., 1984). The strong αN (i, i+1) and $\alpha\delta$ (i, i+1) NOEs (between the non-proline and proline and between two adjacent prolines) leads to an estimate of $\leq$2.2 Å between the respective protons. Such short interproton distances are expected in the ψ region of $\sim$120° $\pm$ 30°, indicating the possible range of backbone ψ angles for all residues. The weak $\alpha\alpha$ (i, i+1) NOEs yield a distance of 4.2−4.4 Å, suggesting the range of ψ_i in the region of $\sim$120° $\pm$ 30°. The presence of the pyrrolidine ring in proline restricts the rotation about the N−C$^\alpha$ bond ($\phi = -60° \pm 15°$ for L-Pro), limiting the freedom of the neighboring group (MacArthur & Thornton, 1991; Hopfinger, 1973), thereby allowing the assignment of the range of ϕ values for Pro residues. For non-proline residues the distance αN (i, i) is dependent on the dihedral angle ϕ_i (Shenderovich et al., 1984; Wüthrich et al., 1984). The major sterically allowed ϕ region for L-residues falls between $\sim$30° and −180° (Wüthrich et al., 1984). The medium and weak αN (i, i) NOEs observed for the non-proline residues are not particularly useful to fix the range of ϕ values. The $J_{NH-C^\alpha H}$ values for the non-proline residues provided in Figure 9 fall in the range of 6.9−7.8 Hz. These values are lower than that expected for fully extended β-strands ($\sim$9 Hz) and higher than that expected for folded α- or 3_{10}-helical (3.9−4.2 Hz) structures (Bystrov, 1976; Wüthrich, 1986; Dyson & Wright, 1991). The $J_{NH-C^\alpha H}$ values of 6.9−7.8 Hz suggest ϕ values of $\sim$−81° to −89° or $\sim$−151° to −159° (Bystrov, 1976; Pardi et al., 1983) for residues other than prolines. Repetitive occurrence of Pro residues in a sequence offers considerable constraint to the peptide backbone by restricting the conformational freedom of the residues preceding and following proline (MacArthur & Thornton, 1991). Therefore, the stereochemical constraints imposed on the non-proline residues flanked by Pro residues indicate only the lower ϕ values of −81° to −89° as the compatible conformational angles. The backbone ϕ angles for non-proline residues are assigned in the range of −81° to −89° $\pm$ 10°. Thus, the NMR studies permit the construction of a crude model using backbone parameters within a certain range.

Since the measured NOE intensities and coupling constants in linear peptides often reflect a population-weighted average over an ensemble of conformations in solution (Dyson & Wright, 1991), the interpretation of coupling constants and NOE data in terms of specific conformations requires extreme caution, especially in the absence of any conformational constraints. The conformational flexibility of the non-proline residues and the reliability of the $J_{NH-C^\alpha H}$ values have been examined by line-shape analysis at various temperatures. The NH resonances at 30 °C shown in Figure 6c are sharp. Decreasing the temperature to 10 °C is expected to lower the rate of chemical exchange across species and perturb the equilibrium of conformational populations resulting in selective line broadening of resonances. However, the line width of NH resonances and coupling constants remain unaltered (Figure 6b) even at 10 °C. This suggests that the non-proline residues are conformationally fairly stable over the temperature range 10−30 °C and the coupling constant values could reflect contributions from a major population of conformers. Selective line broadening and line narrowing of NH and C$^\alpha$H resonances have often been used to delineate conformational flexibility of residues in peptides sequences (Higashijima et al., 1979; Raghothama et al., 1989). It is reasonable to assume that the influence of conformational averaging on $J_{NH-C^\alpha H}$ values and NOE data may not be significant. In the absence of concentration effects the line broadening of NH resonances observed at 40 °C (Figure 4d) presumably indicates chemical exchange between conformers. Since elevated temperature contributes to enhanced chain motion and structural flexibility, it is probable that the major population that is stable at lower temperatures is transforming into higher energy conformers.

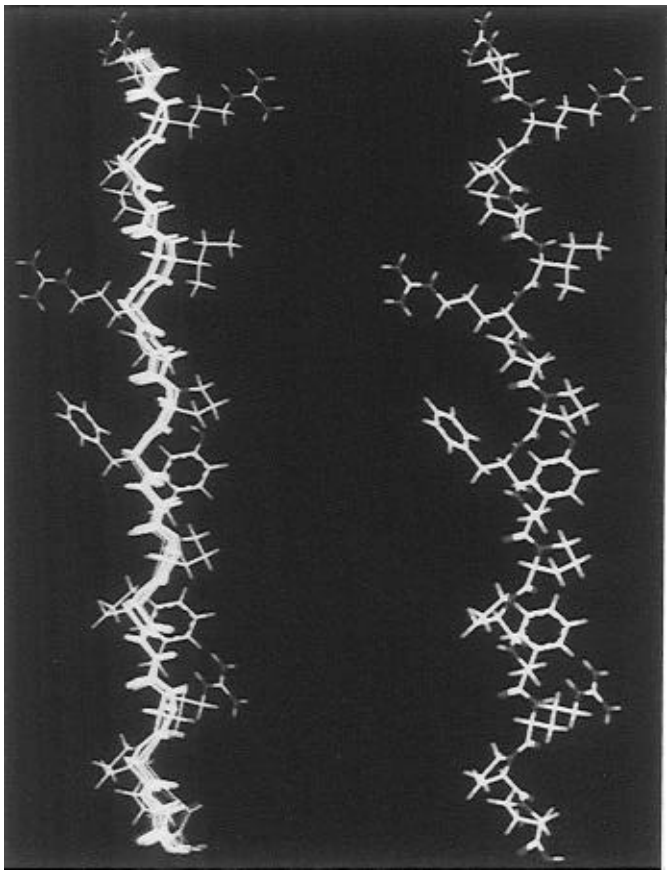

FIGURE 10: Superimposed view of the family of 16 poly(L-proline) II backbone conformations of **BN16** derived from the restrained modeling studies using the NMR and NOE data (left). Perspective view of the averaged poly(L-proline) II structure of **BN16** with the N-terminus at the top and the C-terminus at the bottom (right).

*Molecular Conformation of **BN16***. The superposition of backbones of the family of 16 conformers obtained after energy minimization of DIANA structures, as described in the General Materials and Methods section, is shown in Figure 10. The root mean square deviation (RMSD) between

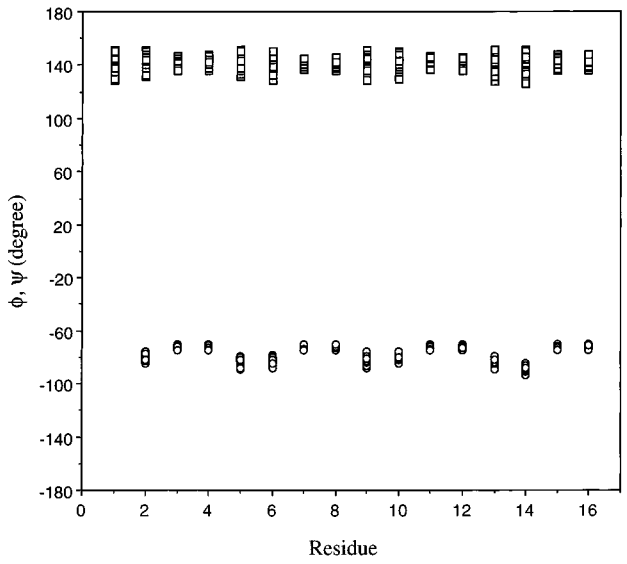

FIGURE 11: Backbone dihedral ϕ (○), ψ (□) in the 16 NMR structures of **BN16**.

the lowest energy conformer and all others ranges from 0.22 to 2.01 Å. The corresponding backbone RMSD ranges from 0.15 to 0.93 Å. The ϕ and ψ angles for the 16 NMR structures are plotted in Figure 11. The ϕ and ψ values of all the 16 structures lie within the conformational space ($\phi = -78° \pm 20°$ and $\psi = 145° \pm 20°$) of poly(L-proline) II. The ϕ values fall in the range of $-70°$ to $-75°$ and $-76°$ to $-92°$ for proline and non-proline residues, respectively. The ϕ values for the non-proline residues in these structures are consistent with the $J_{NH-C^{\alpha}H}$ coupling constants. The ψ values lie between 136° and 147° and between 129° and 151° for proline and non-proline residues, respectively. The average of the 16 structures consistent with the NMR data is shown in Figure 10. The structure is a single-stranded, extended helix with the backbone C═O and NH groups projecting outward. Such single-stranded, extended poly(proline) helical conformations have been observed even in the smaller eight-residue segment of avian pancreatic polypeptide (Blundell et al., 1981). The common occurrence of left-handed poly(proline) II helices in globular proteins, glycoproteins, and synthetic and natural peptides has recently been reported (Makarov et al., 1992; Woody, 1992; Adzhubei & Sternberg, 1993; Sreerama & Woody, 1994).

DISCUSSION

The present study reports the candidacidal activity of bactenecin 5 and its fragments to establish the structure−function relationship of this class of proline-rich polypeptides. The activity data shown in Table 1 indicate that the fragments which have nearly or less than half the size of the parent molecule exhibit cidal potency equivalent to the whole molecule. This seems to indicate that proteolytic degradation of bactenecins expected both *in vivo* and *in vitro* may not significantly lower the fungicidal activity. The fact that **BN16** exhibits the potency of the whole molecule emphasizes this argument. It is pertinent to mention that the cidal potency of the enzymatically degraded fragments of salivary histatins has been found to be comparable to the whole molecule, thereby retaining the antifungal properties of saliva (Xu et al., 1990). When the activity of the fragments of **Bac 5** is compared, the C-terminal fragment **BC24** appears to be less active than the N-terminal fragments at lower concentrations. The **Bac 5** and its N-terminal sequences shown in Figure 1 indicate that the N-terminus is strongly basic due to the presence of Arg_1, Arg_3, and Arg_6, whereas the C-terminus is hydrophobic due to residues such as Pro, Phe, Ile, and Tyr. Though **BC24** has the same number of Arg residues as that of **BN16**, the basic charge is not concentrated at the N-terminus (Figure 1). Collectively, the activity data suggest that a strong basic charge at the N-terminus and a hydrophobic C-terminus may, indeed, be important for eliciting high candidacidal activity. Both **Bac 5** and its fragments have little lytic effect on neutral lipids (Figure 4), whereas their lytic effect on negatively charged lipid vesicles is quite significant as shown in Figure 4, indicating that electrostatic forces could mediate their membrane interaction. The diminished lytic effect observed for the C-terminal fragment **BC24** most probably reflects the decreased positive charge at the N-terminus as compared to the N-terminal fragments. The ability of peptides to lyse the negatively charged lipid vesicles also correlates with their cidal potency. The results seem to indicate that the N-terminus of the peptides may initially interact with the acidic microbial lipid membranes and may lead to the insertion of the hydrophobic C-terminus into the lipid bilayer. However, the present data are not sufficient to ascertain whether these peptides are effective *in vivo* only on negatively charged membranes.

A wide variety of peptide antibiotics have recently been identified and isolated from different biological sources. Examples include histatins (Oppenheim, 1989) in saliva, defensins in neutrophils (Ganz et al., 1985; Selsted et al., 1985), magainins (Erspamer, 1984; Bevins & Zasloff, 1990) in the skin of frogs, and tachyplesins and polyphemusins (Miyata et al., 1989) in hemocytes of horseshoe crabs. Despite their structural variations, their antimicrobial activities are generally related to their efficacy to disrupt microbial membranes. The proline-rich bactenecin peptides appear to exist mostly as poly(L-proline) II helical conformations. The strong negative $\pi-\pi^*$ CD band observed for bactenecin 5 at ~202 nm in aqueous buffer solution and the retention of this band in different solvents of varying polarity and hydrogen-bonding potency provide support to this inference. The CD spectra of bactenecin fragments are also reminiscent of poly(L-proline) II helical conformation, though the ellipticity values are lower than those of the parent molecule. However, as described in the Results section, the CD data cannot distinguish whether the conformational populations are fully extended poly(proline) II helices defined by all residues or Pro-Pro dipeptide segments sandwiched between randomly populated non-proline residues. Nevertheless, similar CD spectra observed for proline-rich polypeptides and oligopeptides have been routinely interpreted in terms of extended poly(proline) II conformations. Examples include the CD studies on histones' C-terminal fragments and β-endorphin (Makarov et al., 1992), repetitive domains of gluteline-2 (Rabanal et al., 1993), and repetitive Gly-$(Pro)_3$ and Gly-$(Pro)_4$ sequences (Helbecque & Lefebvre, 1978).

To examine whether the bactenecin sequences exist in solution as fully extended poly(proline) II or merely Pro-Pro dipeptide segments of poly(proline) II interspaced between non-proline residues in random conformation, we studied the 2D-NMR of **BN16** which retains the activity of the whole molecule and exhibits CD spectra similar to those

of the parent molecule. The coupling constant values and NOE parameters which have been used in the structure elucidation of **BN16** may be complicated by conformational averaging and peptide association especially in linear peptides. The conformational averaging in highly flexible systems can result in NMR-derived virtual conformations which do not correspond to any calculated potential energy minima (Paul et al., 1985, 1987). The presence of even undetectably small amounts of minor conformers has, indeed, been shown to result in selective line broadening in oligopeptides at lower temperatures (Higashijima et al., 1979; Raghothama et al., 1987). The sharp NH resonances observed for **BN16** at 10 °C suggest that the influence of conformational averaging on coupling constants and NOE parameters is not significant and that the non-proline residues in the sequence are fairly conformationally stable. Concentration dependence of NH chemical shifts and the linearity observed for temperature dependence of NH chemical shifts indicate that peptide association is not significant at the concentration used for NMR measurements. Collectively, the data provide support to the implicit assumption that the NOE data and coupling constants are primarily representative of a major conformation. All 16 structures deduced from DIANA using the NMR parameters fall in the conformational space of the poly(L-proline) II conformation ($\phi = -78° \pm 20°$ and $\psi = 145° \pm 20°$). The line broadening effect observed for NH resonances at elevated temperature (40 °C) suggests that the conformationally stable non-proline residues become structurally flexible. This effect may presumably be due to the conformational equilibrium between the ordered poly(proline) II and the disordered random structure. It is also consistent with the red shift of CD bands and the diminished ellipticity observed for these peptides at high temperatures. Similar CD effects have previously been reported for proline-rich peptides (Makarov et al., 1992; Rabanal et al., 1993).

The possibility of other secondary structures being associated with this peptide sequence has been examined by energy calculations. Though the extended β-sheet conformation is energetically favorable, the presence of eight proline residues in the sequence restricts the ϕ values to $-60° \pm 15°$ and the coupling constant values observed for the non-proline residues are lower than that expected for an extended β-sheet. The α-helical conformation involves relatively higher energy and shows the presence of several major steric conflicts between side-chain γ and δ atoms and the backbone atoms of Pro_3, Ile_5, Arg_6, Phe_9, Tyr_{10}, Pro_{12}, Phe_{13}, and Pro_{16}. These observations in addition to the experimental data indicate that the accessible conformational space for the **BN16** sequence is restricted to a poly(proline) II helix.

Of the naturally occurring peptide antibiotics which have been studied so far, only α-helical and β-sheet structures (Lear et al., 1988; Miyata et al., 1989; Bevins and Zasloff, 1990; Kagan et al., 1990) were related to their antimicrobial activity. What is new and novel in this report is that poly(L-proline) II structure also seems to be substantially associated with microbial membrane interaction and antimicrobial activity. The fact that even the shorter sequence **BN16** retains the candidacidal potency of the whole molecule emphasizes the importance of poly(L-proline) II structure for fungicidal activity. Despite the diminished positive charge at the N-terminus, the CD spectra of the C-terminal fragment **BC24** resemble the CD of poly(L-proline) II conformation.

In summary, the results establish that the proline-rich bactenecin 5 and its fragments are powerful candidacidal agents which, unlike other naturally occurring antibiotics, seem to adopt poly(L-proline) II conformation in aqueous and in lipid environment. The N-terminal fragments retain the activity of the whole molecule whereas the C-terminal fragment with a less negative charge at the N-terminus is marginally less active, suggesting the importance of positive charge at the N-terminus. The high content of proline in the sequence seems to stabilize poly(L-proline) II conformations in solution. The observation that the shorter 16-residue sequence (7−22) retains the cidal potency of the whole molecule appears to indicate that in the bactenecin sequence fragments of this size could elicit appreciable candidacidal activity.

ACKNOWLEDGMENT

We acknowledge Dr. A. R. Dentino for his assistance in the purification of bovine neutrophils.

REFERENCES

Adzhubei, A. A., & Sternberg, M. J. E. (1993) *J. Mol. Biol. 229*, 472−493.
Arnott, S., & Dover, S. D. (1968) *Acta Crystallogr. B24*, 599−601.
Baum, B. J., Bird, J. L., & Longton, R. W. (1977) *J. Dent. Res. 56*, 1115−1118.
Bax, A., Byrd, R. A., & Azolos, A. (1984) *J. Am. Chem. Soc. 106*, 7632−7633.
Bevins, C. L., & Zasloff, M. (1990) *Annu. Rev. Biochem. 59*, 395−414.
Blundell, T. L., Pitts, J. E., Tickle, I. J., Woods, S. P., & Wu, C. W. (1981) *Proc. Natl. Acad. Sci. U.S.A. 78*, 4175−4179.
Braunschweiler, L., & Ernst, R. R. (1983) *J. Magn. Reson. 53*, 521−528.
Bystrov, V. F. (1976) *Prog. NMR Spectrosc. 10*, 41−81.
Carver, J. P., & Blout, E. R. (1977) in *Treatise on Collagen* (Ramachandran, G. N., Ed.) Vol. 1, pp 441, Academic Press, New York.
Dyson, H. J., & Wright, P. E. (1991) *Annu. Rev. Biophys. Biophys. Chem. 20*, 519−538.
Epand, R. M., Gawish, A., Iqbal, M., Guptta, K. B., Chen, C. H., Segrest, J. P., & Anantharamaiah, G. M. (1987) *J. Biol. Chem. 262*, 9389−9396.
Erspamer, V. (1984) *Comp. Biochem. Physiol. 79*, 1−7.
Frank, R. W., Gennaro, R., Schneider, K., Przybylski, M., & Romeo, D. (1990) *J. Biol. Chem. 265*, 18871−18874.
Ganz, T., Selsted, M. E., Szklarek, D., Harwig, S. S. L., Daher, K. A., Bainton, D. F., & Lehrer, R. I. (1985) *J. Clin. Invest. 76*, 1427−1435.
Gennaro, R., Dolzani, L., & Romeo, D. (1983) *Infect. Immun. 40*, 684−690.
Gennaro, R., Skerlavaj, B., & Romeo, D. (1989) *Infect. Immun. 57*, 3142−3146.
Güntert, P., & Wüthrich, K. (1991) *J. Biomol. NMR 1*, 447−456.
Güntert, P., Braun, W., & Wüthrich, K. (1991) *J. Mol. Biol. 217*, 517−530.
Helbecque, N., & Lefebvre, M. H. L. (1978) *Int. J. Pept. Protein Res. 11*, 353−362.
Higashijima, T., Inubushi, T., Ueno, T., & Miyazawa, T. (1979) *FEBS Lett. 105*, 337−340.
Hopfinger, A. J. (1973) *Conformational Properties of Macromolecules*, Academic Press, New York.
IUPAC-IUB Commission on Biochemical Nomenclature (1968) *Biochemistry 7*, 2703−2705.
Jeener, J., Meier, B. H., Bachmann, P., & Ernst, R. R. (1979) *J. Chem. Phys. 71*, 4546−4553.
Kagan, B. L., Selsted, M. E., Ganz, T., & Lehrer, R. I. (1990) *Proc. Natl. Acad. Sci. U.S.A. 87*, 210−214.

Kaiser, E., Colescott, R. L., Bossinger, C. D., & Cook, P. I. (1970) *Anal. Biochem. 34*, 595−598.
Kumar, A., Ernst, R. R., & Wüthrich, K. (1980) *Biochem. Biophys. Res. Commun. 64*, 2229−2246.
Laemmli, U. K. (1970) *Nature 227*, 680−685.
Lear, J. D., Wasserman, Z. R., & Degrado, W. F. (1988) *Science 240*, 1177−1181.
Lehrer, R. I., Ganz, T., & Selsted, M. E. (1988) *Haematol. Oncol. Clin. N. Am. 2*, 159−169.
Loomis, R. E., Bergey, E. J., Levine, M. J., & Tabak, L. A. (1985) *Int. J. Pept. Protein Res. 26*, 621−629.
MacArthur, M. W., & Thornton, J. M. (1991) *J. Mol. Biol. 218*, 397−412.
Makarov, A. A., Lobachov, V. M., Adzhubei, I. A., & Esipova, N. G. (1992) *FEBS Lett. 306*, 63−65.
Miyata, T., Tokunaga, F., Yoneya, T., Yoshikawa, K., Iwanaga, S., Niwa, M., Takao, T., & Shimonishi, Y. (1989) *J. Biochem. (Tokyo) 106*, 663−668.
Oppenheim, F. G. (1989) in *Human Saliva: Clinical Chemistry and Microbiology* (Tenovuo, J. O., Ed.) CRC Press, Boca Raton, FL.
Pardi, A., Wagner, G., & Wüthrich, K. (1983) *Eur. J. Biochem. 137*, 445−454.
Paul, P. K. C., & Ramakrishnan, C. (1985a) *J. Biomol. Struct. Dyn. 2*, 879−898.
Paul, P. K. C., & Ramakrishnan, C. (1985b) *Int. J. Pept. Protein Res. 29*, 433−454.
Powell, M. J. D. (1971) *Math. Program 12*, 241−254.
Rabanal, F., Ludevid, M. D., & Giralt, E. (1993) *Biopolymers 33*, 1019−1028.
Raghothama, S., Ramakrishnan, C., Balasubramanian, D., & Balaram, P. (1989) *Biopolymers 28*, 573−588.
Raj, P. A., & Edgerton, M. (1995) *FEBS Lett. 368*, 526−530.
Raj, P. A., Edgerton, M., & Levine, M. J. (1990) *J. Biol. Chem. 265*, 3898−3905.
Raj, P. A., Johnsson, M., Levine, M. J., & Nancollas, G. H. (1992) *J. Biol. Chem. 267*, 5968−5976.
Ronish, E. W., & Krimm, S. (1974) *Biopolymers 13*, 1635−1651.
Scocchi, M. E., Skerlavaj, B., Romeo, D., & Gennaro, R. (1992) *Eur. J. Biochem. 209*, 589−595.
Selsted, M. E., Brown, D. M., DeLange, R. J., Harwig, S. S. L., & Lehrer, R. I. (1985) *J. Biol. Chem. 260*, 4579−4584.
Shenderovich, M. D., Nikiforovich, G. V., & Chipens, G. I. (1984) *J. Magn. Reson. 59*, 1−12.
Sreerama, N., & Woody, R. W. (1994) *Biochemistry 33*, 10022−10025.
States, D. J., Haberkorn, R. A., & Ruben, D. J. (1982) *J. Magn. Reson. 48*, 286−292.
Stewart, J. M., & Young, J. D. (1984) *Solid Phase Peptide Synthesis*, pp 73−95, Pierce Chemical Co., Rockford, IL.
Straubinger, R. M., & Papahadjopoulos, D. (1982) *Methods Enzymol. 101*, 512, 527.
Sundstrom, P. M., Nicols, E. J., & Kenny, G. E. (1987) *Infect. Immun. 55*, 616−620.
Tiffany, M. L., & Krimm, S. (1972) *Biopolymers 11*, 2309−2316.
Vaara, M. (1992) *Microbiol. Rev. 56*, 395−411.
Vijayakumar, E. K. S., Sudha, T. S., & Balaram, P. (1984) *Biopolymers 23*, 877−886.
Weiner, S. J., Kolmann, P. A., Case, D. A., Singh, U. C., Ghio, C., Alagona, G., Profeta, S., Jr., & Weiner, P. (1984) *J. Am. Chem. Soc. 106*, 765−784.
Weiner, S. J., Kollman, P. A., Nguyen, D. T., & Case, D. A. (1986) *J. Comput. Chem. 7*, 230.
Woody, R. W. (1992) *Adv. Biophys. Chem. 2*, 37−79.
Wüthrich, K. (1986) *NMR of Proteins and Nucleic Acids*, John Wiley & Sons, New York.
Wüthrich, K., Billeter, M., & Braun, W. (1984) *J. Mol. Biol. 180*, 715−740.
Xu, T., Telser, R. F., Troxler, R. F., & Oppenheim, F. G. (1990) *J. Dent. Res. 69*, 1717−1723.
Zanetti, M., Litteri, L., Gennaro, R., Horstmann, H., & Romeo, D. (1990) *J. Cell Biol. 111*, 1363−1371.
Zanetti, M., Litteri, L., Griffiths, G., Gennaro, R., & Romeo, D. (1991) *J. Immunol. 146*, 4295−4300.
Zanetti, M., Sal, G. D., Storici, P., Schneider, C., & Romeo, D. (1993) *J. Biol. Chem. 268*, 522−526.

BI951681R